New Phytologist

Research

The three-dimensional construction of leaves is coordinated with water use efficiency in conifers

Santiago Trueba[1,2], **Guillaume Théroux-Rancourt**[3], **J. Mason Earles**[4], **Thomas N. Buckley**[5], **David Love**[6], **Daniel M. Johnson**[6] **and Craig Brodersen**[1]

[1]School of the Environment, Yale University, New Haven, CT 06511, USA; [2]University of Bordeaux, INRAE, UMR BIOGECO, Pessac 33615, France; [3]University of Natural Resources and Life Sciences, Vienna, Department of Integrative Biology and Biodiversity Research, Institute of Botany, Vienna 1180, Austria; [4]Department of Viticulture and Enology, University of California, Davis, CA 95616, USA; [5]Department of Plant Sciences, University of California, Davis, CA 95916, USA; [6]Warnell School of Forestry and Natural Resources, University of Georgia, Athens, GA 30602, USA

Author for correspondence:
Santiago Trueba
Email: strueba@gmail.com;

Received: *25 May 2021*
Accepted: *21 September 2021*

New Phytologist (2022) **233:** 851–861
doi: 10.1111/nph.17772

Key words: carbon assimilation, conifers, gas exchange, gymnosperms, leaf anatomy, stomatal conductance, stomatal density, water use efficiency.

Summary

- Conifers prevail in the canopies of many terrestrial biomes, holding a great ecological and economic importance globally. Current increases in temperature and aridity are imposing high transpirational demands and resulting in conifer mortality. Therefore, identifying leaf structural determinants of water use efficiency is essential for predicting physiological impacts due to environmental variation.
- Using synchrotron-generated microtomography imaging, we extracted leaf volumetric anatomy and stomatal traits in 34 species across conifers with a special focus on *Pinus*, the richest conifer genus.
- We show that intrinsic water use efficiency (WUE_i) is positively driven by leaf vein volume. Needle-like leaves of *Pinus*, as opposed to flat leaves or flattened needles of other genera, showed lower mesophyll porosity, decreasing the relative mesophyll volume. This led to increased ratios of stomatal pore number per mesophyll or intercellular airspace volume, which emerged as powerful explanatory variables, predicting both stomatal conductance and WUE_i.
- Our results clarify how the three-dimensional organisation of tissues within the leaf has a direct impact on plant water use and carbon uptake. By identifying a suite of structural traits that influence important physiological functions, our findings can help to understand how conifers may respond to the pressures exerted by climate change.

Introduction

Conifer forests thrived on the Earth surface during the Mesozoic period until the radiation and diversification of angiosperms during the Cretaceous, which was followed by angiosperm ecological dominance attributed to increased physiological performance and reduced generation times (Bond, 1989; Boyce *et al.*, 2009; Crepet & Niklas, 2009; de Boer *et al.*, 2012). Yet, after 100 Myr of competition with the angiosperms, conifers remain prominent in the canopy of many biomes (Brodribb *et al.*, 2012). Conifers are found in ecosystems from high latitudes to the equator, and they have major economic importance in the wood and paper industries (McFarlane & Sands, 2013). Conifer-dominated forests are not exempt from the impacts of drought and aridity resulting from ongoing global climatic changes (Dai, 2011; Brodribb *et al.*, 2020; Kharuk *et al.*, 2021). This is particularly alarming given that 48% of the 722 conifer taxa of the world are currently under threat (Blackmore *et al.*, 2011). Global increases in temperature coupled with rising vapour pressure deficit (VPD) place increased strain on plant hydraulic and photosynthetic systems (Choat *et al.*, 2018; Grossiord *et al.*, 2020). There is strong evidence that tree water use efficiency (WUE) has increased in recent decades, most probably the result of rising atmospheric CO_2, allowing plants to open their stomata less frequently, thereby conserving water (Keenan *et al.*, 2013; Mathias & Thomas, 2021). However, the underlying physiological mechanisms behind this trend need to be further elucidated (Guerrieri *et al.*, 2019). Furthermore, there is still a lack of knowledge on how leaf structural organisation influences key functions such as photosynthetic carbon acquisition, stomatal conductance, and the interplay between both driving intrinsic water use efficiency (WUE_i).

Leaf-level photosynthetic metabolism has an important role in maintaining global ecological processes (Hetherington & Woodward, 2003). Therefore, exploring tissue organisation inside the leaf, and specifically the mesophyll cells where water and gas diffusion occur, is important for understanding carbon, water and energy fluxes at whole ecosystem levels. The leaf mesophyll consists of photosynthetic parenchyma cells located between the epidermis and the endoderm and transfusion tissue layers that surround the veins. Once inside the leaf, diffusion of CO_2 from the intercellular airspace (IAS) to the chloroplast stroma (i.e. mesophyll conductance) is a major constraint on photosynthetic performance (Flexas *et al.*, 2012; Gago *et al.*, 2020). This pathway includes the IAS, but also the diffusion of CO_2 across mesophyll cell walls, cell membranes and the chloroplast envelope, which can significantly limit photosynthesis in gymnosperms (Carriquí *et al.*, 2020). Previous work has shown that mesophyll surface area per leaf area (S_m; $\mu m^2\,\mu m^{-2}$) has a strong influence on maximum photosynthesis (Nobel *et al.*, 1975; Smith & Nobel, 1977). More recently, it has been suggested that the surface area of the mesophyll exposed to the IAS per unit of mesophyll volume (SA_{mes}/V_{mes}; $\mu m^2\,\mu m^{-3}$) can influence plant photosynthetic performance given that the mesophyll-IAS boundary is the primary interface between the atmosphere and the photosynthetic cells (Earles *et al.*, 2018; Théroux-Rancourt *et al.*, 2021). Other volumetric anatomical traits such as mesophyll porosity (i.e. IAS as a fraction of total mesophyll volume; $\mu m^3\,\mu m^{-3}$) might be relevant in promoting diffusion through the IAS, and it has been suggested that mesophyll palisade porosity is correlated with stomatal conductance across four different *Arabidopsis* mutants (Lundgren *et al.*, 2019). The relevance of such anatomical traits arises from the hypothesis that photosynthetic capacity could be enhanced by increasing surface area of mesophyll exposed to the IAS, allowing for more potential surface for CO_2 diffusion across mesophyll cell walls, and chloroplast envelopes (Evans *et al.*, 2009; Earles *et al.*, 2018). However, the correct estimation of such anatomical traits using standard two-dimensional (2D) techniques is difficult as it relies on 2D approximations of the complex, three-dimensional (3D) shape of the mesophyll (Théroux-Rancourt *et al.*, 2017; Earles *et al.*, 2019).

Given the elementary vascular architecture of the conifer leaf, which typically consists of a single vein without further branching (Zwieniecki *et al.*, 2004; Brodribb *et al.*, 2010), and the large variation in conifer leaf shape (Fig. 1), area-based traits might not allow for an accurate comparison of strategies to optimise leaf structure with function within conifers (Earles *et al.*, 2019; Théroux-Rancourt *et al.*, 2021). Furthermore, given the structural relevance of the central vasculature, traits other than those related to the mesophyll might also influence CO_2 and water diffusion in the conifer leaf. Therefore, a central question is whether nonvascular tissues are tightly coupled to vein volume with proportional relationships, or whether they show greater variability to compensate for reduced hydraulic efficiency. We predict that higher volumes of vascular tissue per unit leaf volume (V_{vein}/V_{leaf}; $\mu m^3\,\mu m^{-3}$) should be a good predictor of gas exchange and WUE_i because of the mechanistic link between hydraulic conductance and maximum photosynthetic rates in conifers (Brodribb & Feild, 2000). We also predict a positive relationship between gas exchange efficiency and the ratio of mesophyll surface area exposed to the IAS and vein volume (SA_{mes}/V_{vein}; $\mu m^2\,\mu m^{-3}$), where a greater investment in vein volume per unit area of bulk tissue surface should increase the hydraulic capacity to replace water lost to transpiration. In conifer leaves, water moves across the transfusion tissue and a ring of parenchymatous sheath cells or an endoderm before reaching the mesophyll (Hu & Yao, 1981). Therefore, transfusion tissue and endoderm volume relative to total leaf volume (V_{TT+en}/V_{leaf}; $\mu m^3\,\mu m^{-3}$), should also influence the efficiency of water movement within the leaf. Along with the previously described features, many conifer species also possess resin ducts, which play a major role in chemical and physical defence (Gaylord *et al.*, 2013; Breshears *et al.*, 2018), but necessarily displace vascular or photosynthetic tissue, incurring both maintenance and construction costs, but also lost opportunity costs for net carbon gain. Finally, water movement inside the leaf ends at the stomatal pores, which play a major role in regulating water loss and maintaining water status

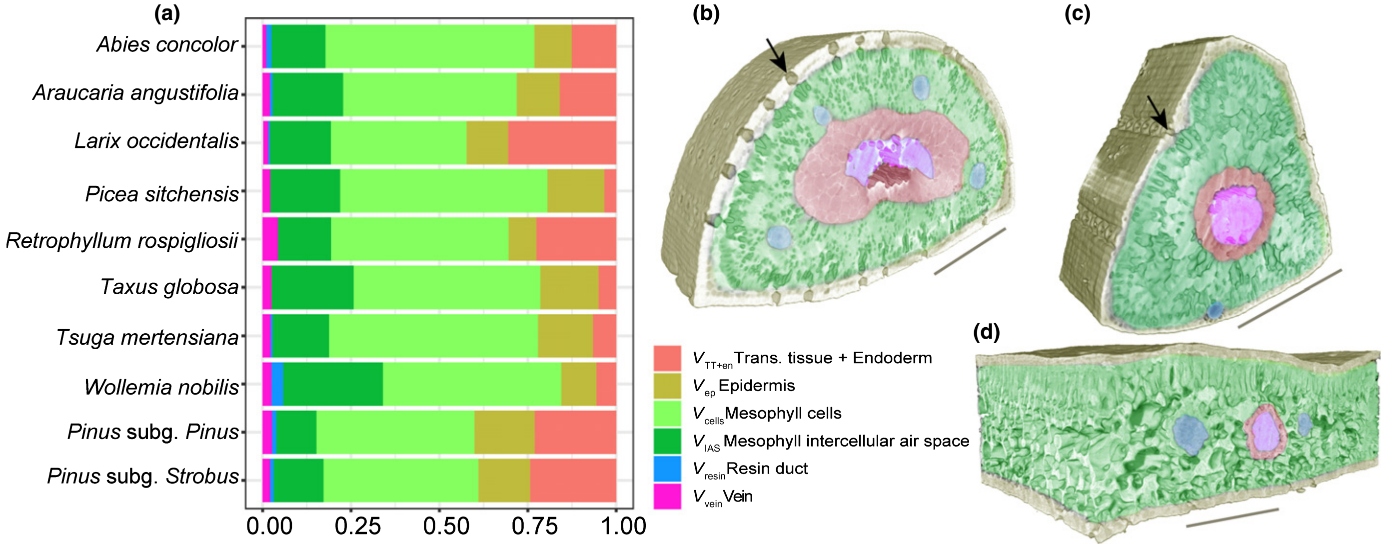

Fig. 1 Proportion of different tissue volumes relative to total leaf volume inside the 3D leaf space in conifers (a). Average values of *Pinus* species belonging to the *Pinus* (21 spp.) and *Strobus* (5 spp.) subgenera are included. Microtomography 3D images of needle-leaved *Pinus pungens* (b; *Pinus* subgenus) and *Pinus monticola* (c; *Strobus* subgenus) and flat-leaved *Wollemia nobilis* (d). Segmented tissues are indicated with different colours and stomatal apertures are indicated with arrows. Bars, 250 μm. A plot of the relative tissue volume of all 34 species is available in Supporting Information Fig. S2.

in conifers (Brodribb *et al.*, 2014). Within this context, it is possible to determine the proportionality of different anatomical traits, the coordination between supply and demand for CO_2 and H_2O, and the physical constraints of leaf construction. To probe these relationships, we describe how conifers build their elementary, yet diverse leaves, and how structural features relate to key physiological traits.

This study presents a survey of the three-dimensional organisation of the conifer leaf using microtomography (microCT) imaging (Supporting Information Table S1). Our study includes 34 conifer species (Fig. S1), with a special focus on the genus *Pinus*, the largest extant genus of conifers (Gernandt *et al.*, 2005). *Pinus* species can be found in a broad range of environmental conditions, suggesting wide structural and functional diversity (Martínez-Vilalta *et al.*, 2004). *Pinus* subgenera *Pinus* and *Strobus* can be distinguished by having two or one vascular bundles respectively, centrally located inside the needle-like leaf (Gernandt *et al.*, 2005) (Fig. 1a–c). Despite their rather simple anatomical organisation, conifer leaves have extensive morphological diversity ranging from flat leaves to needle-like leaves with different degrees of transversal flattening. Leaf morphological diversity in conifers results in different physiological performances, with flat-leaved species having lower photosynthetic assimilation and respiration rates than needle-leaved species (Brodribb & Feild, 2008; Schmiege *et al.*, 2020, 2021). Yet, the differences in 3D anatomical structure across conifers with different leaf morphologies, which could explain their contrasting photosynthetic performance, need to be elucidated. We hypothesise that features enhancing mesophyll surface area for gas diffusion, will be positively correlated with the light-saturated assimilation rate of CO_2 (A_{sat}) and stomatal conductance (g_s). We also provide a volume-based stomatal density estimation, a trait we expect better captures the interplay between the evaporative surfaces invested in the nonlaminar mesophyll volume and the number of stomata needed to provide CO_2, with the expectation that leaves with higher number of stomata per mesophyll volume would have both higher rates of gas exchange and WUE_i due to an enhancement of the epidermal pores serving as evaporative surface relative to the photosynthetic tissue.

Materials and Methods

Plant material

Sampling included 34 conifer species from various biomes, physiologies and leaf morphologies. Sampling included taxa from four different families of conifers: Araucariaceae (2 spp.), Pinaceae (30 spp.), Podocarpaceae (1 sp.), and Taxaceae (1 sp.). Our sampling particularly focused on the genus *Pinus* with 26 species including representatives from the two subgenera: *Pinus* (21 spp.) and *Strobus* (5 spp.), which differ in the number of vascular bundles per leaf (Gernandt *et al.*, 2005). Sampling also represents three distinct conifer leaf morphologies: flat leaves (*Araucaria*, *Retrophyllum*, *Taxus* and *Wollemia*; Fig. 1d), flattened needles (*Abies*, *Larix*, *Picea* and *Tsuga*), and needle-like leaves (*Pinus*; Fig. 1b,c). Flattened needles, such as those commonly found in non-*Pinus* Pinaceae, are generally shorter and flattened in cross-section compared with *Pinus* needle-like leaves, which have almost equal width and height (Fig. 1b,c) and are generally longer. Fully expanded leaves from adult plants were collected in the Berkeley Arboretum of the University of California Botanical Garden, and the University of Georgia's Thompson Mills Arboretum. Samples from both locations were used for microCT scanning and gas exchange measurements. Whole shoots were cut, wrapped in moist paper towels, and transported in dark plastic bags to avoid desiccation before scanning.

X-ray microtomography scanning and image segmentation

Microtomography imaging was performed at the Lawrence Berkeley National Laboratory Advanced Light Source, beamline 8.3.2. Leaves were scanned at the mid-section within 24 h of excision. Two replicates were scanned for 18 species, while a single leaf was scanned for the remaining 16 species (Dataset S1). Samples were wrapped with polyimide tape, which allows X-ray transmittance while preventing sample desiccation. Wrapped leaf samples were placed in a plastic 1000 µl pipette tip with the lower end submerged in water and centred in the microCT X-ray beam. Scans were completed in *c.* 15 min in continuous tomography mode at 21 keV capturing 1025 projection images of 200–250 ms each. Images were captured using alternatively ×5 or ×10 objective lenses depending on leaf diameter, yielding final pixel resolutions of 1.27 and 0.625 µm. Images were reconstructed using TomoPy (Gürsoy *et al.*, 2014). Raw tomographic datasets were reconstructed using both gridrec and phase retrieval methods, both of which yield complementary results being efficient in segmenting cell boundaries and larger air voids, respectively (Théroux-Rancourt *et al.*, 2017). Image stacks of *c.* 2600 8-bit greyscale images were generated from the reconstruction process. Airspace was segmented in both gridrec and phase reconstruction methods by visually defining a range of pixel intensity values and the binary image stacks from both reconstruction methods were combined. Boundaries delimiting the areas occupied by the endoderm + transfusion tissue, epidermis, mesophyll, resin ducts, and veins were manually drawn using a graphic tablet (Wacom Cintiq Pro 16; Wacom Co, Saitama, Japan) using ImageJ software (Schneider *et al.*, 2012). Leaf veins were depicted here as the vascular bundle comprising both xylem and phloem tissues. Leaf tissue boundaries were drawn as regions of interest in six to eight images randomly distributed across the full stack. The combination of the binary image derived from both reconstruction methods, along with the tissue boundaries, resulted in a composite image stack where each leaf tissue was classified. Leaf segmentation, which allowed us to automatically delimit different tissues across the full stack using a limited set of hand-segmented composite slices was done using random-forest classification (Théroux-Rancourt *et al.*, 2020).

Three-dimensional anatomy and stomatal traits

We extracted the volume and surface area of leaf anatomical traits from the full segmented stacks (Théroux-Rancourt *et al.*, 2020).

We estimated the volume of the epidermis and hypodermis (V_{ep}), which were segmented together when hypodermal cell layers were present, due to the proximity of both peripheral tissues. Mesophyll cells (V_{cell}) and mesophyll IAS (V_{IAS}) were estimated independently, and mesophyll volume (V_{mes}) was estimated as the sum of V_{cell} and V_{IAS}. Conifer leaves have an endoderm (Lersten, 1997) or a uniseriate ring of parenchymatous sheath cells that surrounds the transfusion tissue. Transfusion tissue, a common feature of gymnosperm leaves, is located between the sheath cells and the veins, and it is composed of transfusion tracheids, transfusion parenchyma, and albuminous cells (Hu & Yao, 1981). We estimated the volume of the ensemble conformed by the transfusion tissue and the adjacent endoderm (V_{TT+en}). Furthermore, we estimated the volume of resin ducts (V_{resin}), and veins (V_{vein}). All volume metrics are reported in μm^3. Relative volumes for each tissue (in $\mu m^3\ \mu m^{-3}$) were estimated as a fraction of tissue per V_{leaf}, total leaf volume, which corresponds to the sum of the surface of the leaf cross-section on each slice multiplied by slice depth across the full stack. We calculated mesophyll porosity ($\mu m^3\ \mu m^{-3}$) as V_{IAS}/V_{mes}. The mesophyll surface area exposed to the IAS (SA_{mes}) was used to estimate the mesophyll surface area per mesophyll volume (SA_{mes}/V_{mes}; $\mu m^2\ \mu m^{-3}$). Additionally, we estimated the exposed mesophyll surface area per transfusion tissue + endoderm volume (SA_{mes}/V_{TT+en}; $\mu m^2\ \mu m^{-3}$) and vein volume (SA_{mes}/V_{vein}; $\mu m^2\ \mu m^{-3}$). Total leaf area A_{leaf} (μm^2) was measured by summing up the perimeter of each slice and multiplying it by slice depth. We used the ratio SA_{mes}/A_{leaf} to calculate the mesophyll surface area per total leaf area (S_m; $\mu m^2\ \mu m^{-2}$). Stomatal estimations were performed by counting all visible stomata on the leaf surface of each scan using AVIZO 9.4 software (FEI Co., Hillsboro, OR, USA). Absolute stomatal counts were used in relation to mesophyll volumetric anatomy to estimate traits accounting for the interaction of stomata pore number and V_{IAS}, V_{mes} and SA_{mes} units. Mesophyll volumetric features were assessed in mm^3 for stomatal pore density estimations. We also accounted for stomatal number per leaf surface to assess potential differences in stomatal density estimations based on surface vs volume fractions. Furthermore, we performed a comparison of surface- and volume-based anatomical estimations using 2D slices and the full 3D stack. Methods are further explained in Notes S1. Average trait values for each species are available in Dataset S1. A list of measured anatomical variables, including abbreviations and units, is available in Table S1.

Gas exchange and WUE measurements

Stomatal conductance (g_s; mmol $m^{-2}\ s^{-1}$) and light-saturated CO_2 assimilation rate (A_{sat}; µmol $m^{-2}\ s^{-1}$) were measured on a subset of 18 species (Dataset S1) and used to estimate leaf-level intrinsic water use efficiency ($WUE_i = A_{sat}/g_s$; µmol mol^{-1}). A_{sat} data for *Pinus strobus* were removed before analyses due to potential measurement inaccuracies. Gas exchange measurements were performed on 3–5 individuals for each species with a Li-Cor-6800 gas exchange system (Li-Cor Biosciences, Lincoln, NE, USA) between 09:00 h and 14:00 h on fully sunlit outer canopy foliage. Chamber temperature was set to 25°C, light source was set to 1500 µmol $m^{-2}\ s^{-1}$ and chamber CO_2 was set to 400 ppm. Following the gas exchange measurements, the leaf area contained within the chamber was marked using a permanent marker, collected, and the projected leaf area was measured using a leaf area meter (LI3100C; Li-Cor Biosciences).

Data analysis

All statistical analyses and data treatment were performed using R v.3.6.3 (R Core Team, 2020). Anatomical traits were assembled and averaged for each species for data analysis. Assumptions for residual homogeneity and normality were tested before data analyses. Phylogenetic relationships, including branch length calibrations and divergence times, were obtained from published data (Magallón *et al.*, 2015; Smith & Brown, 2018). To predict leaf physiological traits based on volumetric anatomical variables we used phylogenetic generalised least-squares analyses (PGLS) with a lambda (λ) maximum likelihood optimisation to control for phylogenetic nonindependence between related species (Felsenstein, 1985; Freckleton *et al.*, 2002). A two-parameter exponential function, $y = a(1 - \exp(-bx))$, was additionally used to describe the relationship of WUE_i and V_{vein}/V_{leaf} ($a = 130$, $b = 109$, $r^2 = 0.50$). The assemblage of the composite phylogenetic tree of studied conifers (Dataset S2) was carried out using the package APE (Paradis & Schliep, 2019) and PGLS models were fit using the package CAPER (Orme *et al.*, 2018). Standard major axes (SMA) were implemented with the package SMATR (Warton *et al.*, 2012) to test allometric scaling between tissue volumes. A principal component analysis (PCA) was used to explore the covariation of selected traits and the distribution of leaf morphologies and conifer groups as explained by the physiological and anatomical traits measured. Given the marked differences in leaf anatomical structure across conifer leaf morphological types, and between *Pinus* subgenera *Pinus* and *Strobus*, we explored potential variation in 3D anatomical traits by plotting each group within the PCA. We further explored differences across leaf morphologies and between conifer clades by performing a one-way ANOVA on measured structural traits. Physiological features were not compared between leaf morphological types due to insufficient data availability. A similar variance meta-analysis, including post hoc Tukey's honest significant differences, was used to compare the studied conifer species with other gymnosperms, along with angiosperms and ferns. Data for comparisons across plant groups were obtained from a recently published study (Théroux-Rancourt *et al.*, 2021) and are available in Dataset S3.

Results

The mesophyll (V_{mes}/V_{leaf}), including cells and airspace, represents the dominant leaf volume fraction for all 34 measured conifer species in this study, occupying an average of 60% of the total leaf volume (Figs 1, S2). The second largest volume fraction was either the combined transfusion tissue and endoderm (V_{TT+en}/V_{leaf}) that surrounds the vascular cylinder, or the epidermis (V_{ep}/V_{leaf}), which represented an average of 22% and 16% of the leaf volume, respectively (Fig. 1a). Veins (V_{vein}/V_{leaf}) and resin ducts (V_{resin}/V_{leaf}) represented the smallest fraction of the total leaf volume (Fig. 1a), and resin ducts were completely absent in six measured species (Dataset S1). We found weak structural coordination amongst tissue volumes within the conifer leaf (SMA; Table S2). However, a negative allometric scaling between V_{ep}/V_{leaf} and V_{mes}/V_{leaf} was observed ($r^2 = 0.27$, $P < 0.01$), indicating that increasing the relative allocation to the mesophyll was done in conjunction with a decrease in the relative allocation to the epidermis. Average values of all measured volumetric traits for each species are included in Dataset S1.

A multivariate analysis of trait covariation defined two major axes explaining 48% of inertia (Fig. 2). Inertia of the first axis was mainly explained by V_{IAS}/stomate, the amount of air volume connected to a stomate (18.27%), stomata/V_{mes}, the stomatal density per mesophyll volume (15.04%), V_{mes}/V_{leaf} (14.74%) and g_s (14.08%). Increasing g_s was associated on the first axis with increases in stomata/V_{mes} and A_{sat}, and decreases in mesophyll porosity, V_{mes}/V_{leaf}, and V_{IAS}/stomate (Fig. 2). The second axis was largely explained by V_{vein}/V_{leaf} (18.04%), SA_{mes}/V_{vein} (14.83%) and S_m (14.45%). Increasing WUE$_i$ was associated on the second axis with increases in S_m and V_{vein}/V_{leaf}, and decreases in stomata/V_{mes} (Fig. 2). Leaf morphological types were dispersed along both major axes (Fig. 2). Needle-like leaves were isolated due to their higher V_{ep}/V_{leaf} and stomata/V_{mes}. Flat leaves and flattened needles largely overlapped due to their porous and voluminous mesophylls as opposed to needle-like leaves (Fig. 3a,b). Flat leaves and flattened needles also converged in having lower stomata/V_{mes} (Fig. 3c) and higher V_{IAS}/stomate (Fig. 3d) than needle-like leaves. However, flattened needles were differentiated due to some species having significantly higher SA_{mes}/V_{vein} (Fig. 2; Table S3). Conifer groups were also effectively segregated based on their volumetric anatomy. Non-*Pinus* conifer species were segregated on the first axis (Fig. 2) due to their higher porosity (Fig. 1d), V_{mes}/V_{leaf}, and V_{IAS}/stomate values, while species from the *Pinus* subgenus were grouped (Fig. 2) due to higher V_{ep}/V_{leaf} (Fig. 1b), along with a relatively larger SA_{mes}/V_{mes}. Species from the *Strobus* subgenera were located between the

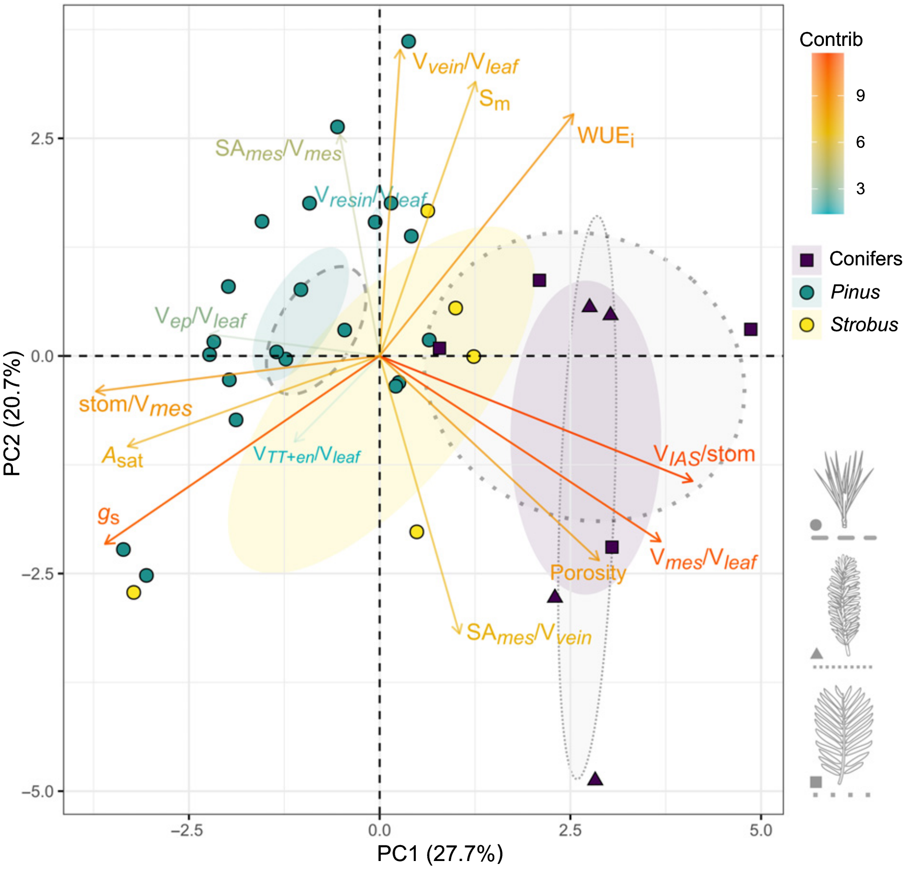

Fig. 2 Principal component analysis (PCA) of physiological and volumetric anatomy traits of conifer species. Arrows and trait colour gradients indicate the contribution of each variable to the axes. Species from the two *Pinus* subgenera, along with other studied conifer species are indicated in different colours, and 95% confidence ellipses are included. Confidence ellipses for different leaf morphologies are also included. Species bearing flat leaves (squares, dotted line), flattened needle leaves (triangles, narrow dotted line), and needle-like leaves (circles, dashed line) are identified. A_{sat}, light-saturated photosynthetic assimilation rate; g_s, stomatal conductance; Porosity, mesophyll porosity; SA_{mes}/V_{mes}, mesophyll surface area per unit mesophyll volume; SA_{mes}/V_{vein}, mesophyll surface area per unit vein volume; S_m, mesophyll surface area per total leaf area; stom/V_{mes}, stomatal pore number per unit mesophyll volume; V_{ep}/V_{leaf}, epidermis volume relative to total leaf volume; V_{IAS}/stom, intercellular airspace volume per stomate; V_{mes}/V_{leaf}, mesophyll volume relative to total leaf volume; V_{resin}/V_{leaf}, resin duct volume relative to total leaf volume; V_{TT+en}/V_{leaf}, transfusion tissue and endoderm volume relative to total leaf volume; V_{vein}/V_{leaf}, vein volume relative to total leaf volume; WUE$_i$, intrinsic water use efficiency.

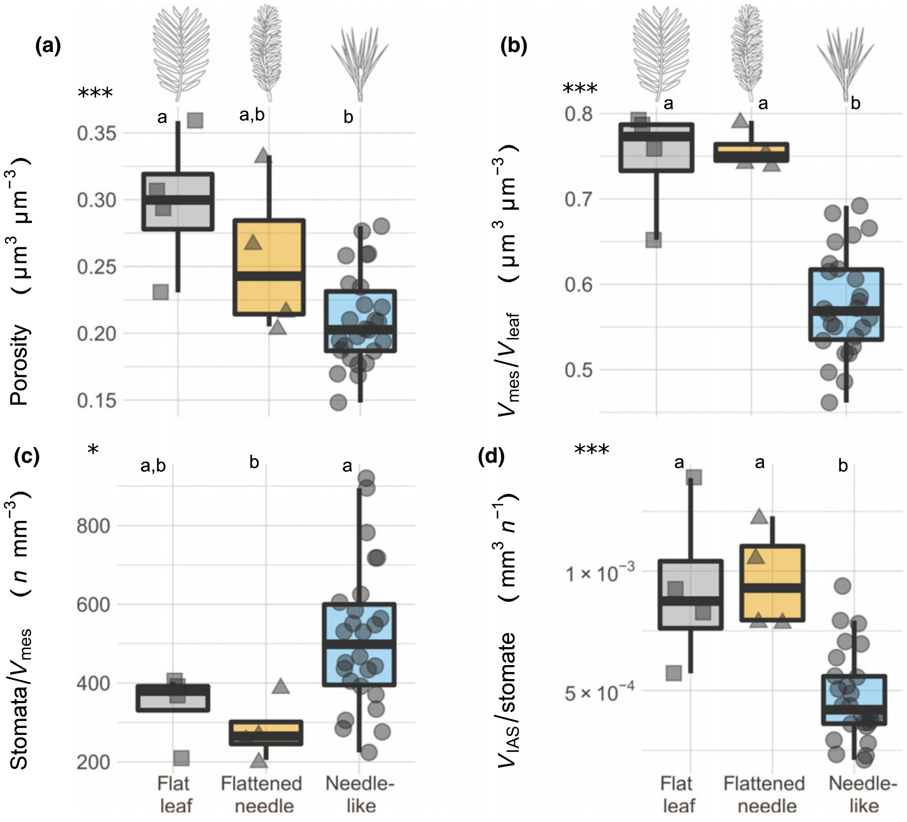

Fig. 3 Differences in mesophyll volumetric traits (a, b) and stomatal features (c, d) across flat (squares), flattened needle (triangles) and needle-like (circles) leaves in the conifer species studied. Horizontal lines, boxes and bars show the median, quartiles and extreme values, respectively. Grey dots are species data points. *P*-value notations represent results of one-way ANOVAs between groups. *, $P \leq 0.05$; ***, $P \leq 0.001$. Letters indicate significant differences between leaf morphological types. Furthermore information and other comparisons of anatomical traits across leaf morphology types are available in Supporting Information Table S3. Porosity, mesophyll porosity; stomata/V_{mes}, stomatal pore number per unit mesophyll volume; V_{IAS}/stomate, intercellular airspace volume per stomate; $V_{\mathrm{mes}}/V_{\mathrm{leaf}}$, mesophyll volume relative to total leaf volume.

previously described conifer groups (Fig. 2). Structural divergences of leaf morphologies, distinguishing three distinct functional groups, along with the segregation of different conifer clades in the PCA analysis were further supported with one-way ANOVA analyses on 3D leaf anatomical traits and stomatal density (Tables S3, S4). Relative vein volume and $\mathrm{SA}_{\mathrm{mes}}/V_{\mathrm{mes}}$ were highly conserved (Fig. S3; Tables S3, S4), whereas $\mathrm{SA}_{\mathrm{mes}}/V_{\mathrm{vein}}$, along with traits related to the ratio of stomatal pore number and mesophyll tissue volumes had significant differences across both leaf morphologies and conifer groups (Figs 3c,d, S3; Tables S3, S4).

To explore the functional implications of 3D tissue content, we determined their relationships to gas exchange parameters such as A_{sat}, g_s and WUE_i. WUE_i was best predicted by $V_{\mathrm{vein}}/V_{\mathrm{leaf}}$ (Fig. 4a), where higher $V_{\mathrm{vein}}/V_{\mathrm{leaf}}$ enhances leaf WUE_i. Furthermore, 2D anatomical estimations of the ratio $A_{\mathrm{vein}}/A_{\mathrm{leaf}}$ were comparable with $V_{\mathrm{vein}}/V_{\mathrm{leaf}}$, extracted using a 3D approach (Notes S1; Fig. S4). The mesophyll surface area exposed to vein volume ($\mathrm{SA}_{\mathrm{mes}}/V_{\mathrm{vein}}$) was also an accurate predictor and showed a negative relationship with WUEi (Fig. 4b). A positive relationship of WUE_i with S_m was also found using generalised least-square models corrected for phylogenetic relatedness (PGLS) analyses (Table S5). A_{sat} was the physiological trait showing the least linkage with 3D structural traits. However, we found a negative relationship between A_{sat} and mesophyll porosity along with $V_{\mathrm{mes}}/V_{\mathrm{leaf}}$ (Fig. S5a), suggesting that conifer species with lower relative mesophyll volumes have greater photosynthetic assimilation rates. Additionally, V_{IAS}/stomate was also negatively related to A_{sat} (Fig. S5b). The number of stomata per unit mesophyll tissue volume predicted g_s and WUE_i (Fig. 5). For instance, high stomatal densities relative to mesophyll volume (stomata/V_{mes}) enhanced g_s (Fig. 5a) while decreasing WUE_i (Fig. 5b). Evolutionary coordination between leaf volumetric anatomy and physiological traits was supported by PGLS analyses (Table S5). Stomatal density measured on a 2D leaf surface area basis (stomata/A_{leaf}), included here as a reference of a more standard approach, did not relate to any physiological trait (Table S5). Therefore, the interaction of mesophyll volume and stomatal pore numbers emerged as a key trait to explain leaf physiological performance (Fig. 5). A comparison of the studied conifers with published data for other gymnosperm species, along with angiosperms and ferns, showed that conifers had fewer stomata per unit mesophyll volume than angiosperms *sensu largo* (Fig. S6; Dataset S3). However, this difference was less important when considering evergreen angiosperms alone. Conifers showed a similar stomata/V_{mes} ratio as other gymnosperm species and ferns (Fig. S6).

Discussion

Conifers, with their long-lasting and anatomically elementary leaves, must rely on leaf construction to enable sufficient carbon assimilation to survive and reproduce while limiting water loss. However, the simple design of coniferous leaves has been considered to have a poor, if not absent, hydraulic connection between the vein xylem and the bulk leaf tissue (Zwieniecki *et al.*, 2007).

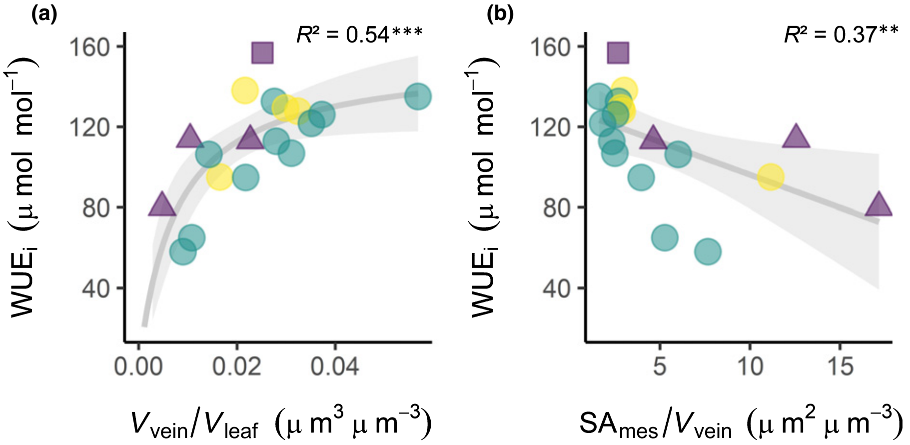

Fig. 4 Water use efficiency (WUE$_i$) as a function of vein volumetric traits of conifer leaves. Relationships of WUE$_i$ with relative vein volume (a) and the surface area of the mesophyll exposed to the intercellular airspace per unit of vein volume (b) across 18 conifer species. Solid regression lines and 95% confidence intervals (grey shaded areas) are included. *Pinus* species from the subgenera *Pinus* (green) and *Strobus* (yellow), along with other conifer species (purple) are indicated. Species bearing flat leaves (square), flattened needle leaves (triangles), and needle-like leaves (circles) are also identified. Phylogenetic generalised least-squares coefficients of determination are included. **, $P < 0.01$; ***, $P < 0.001$. Additional information is available in Supporting Information Table S5.

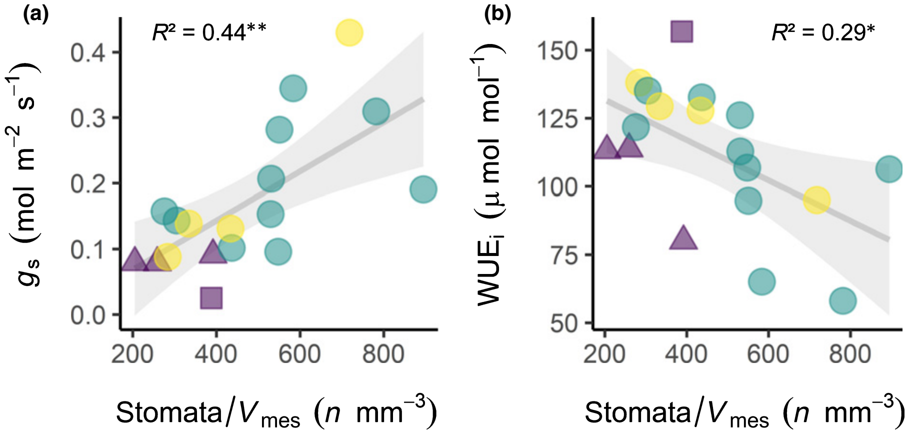

Fig. 5 Physiological traits explained by volumetric stomatal density in conifer leaves. Relationships of stomatal conductance (a) and water use efficiency (b) with the number of stomata per unit of mesophyll volume across 18 conifer species. Solid regression lines and 95% confidence intervals (grey shaded areas) are included. *Pinus* species from the subgenera *Pinus* (green) and *Strobus* (yellow), along with other conifer species (purple) are indicated. Species bearing flat leaves (square), flattened needle leaves (triangles), and needle-like leaves (circles) are also identified. Phylogenetic generalised least-squares coefficients of determination are included. *, $P < 0.05$; **, $P < 0.01$. Additional information available in Supporting Information Table S5.

This is unsurprising as conifer leaves are not as fully vascularised as those of angiosperms and present a single cohort of relatively inefficient leaves (Bond, 1989). The likely consequence of this poor hydraulic connection is a larger difference in water potential between the veins and the mesophyll and epidermis in transpiring leaves, which may force stomata to close even when water potential is relatively high in the veins (Zwieniecki *et al.*, 2007). Our results show that, despite occupying a small fraction (*c.* 2%) of the leaf volumetric matrix, vein tissue volume has a great impact on the leaf WUE$_i$ (Fig. 4a). As the relative vein volume expands, the space between the vascular tissues and the bulk leaf tissues become smaller, potentially reducing the hydraulic resistance for water transport from the vasculature to the bulk leaf. Our study provides an estimation of the full volumetric space occupied by the vein tissue relative to the photosynthetic cells. While we consider volumetric estimates to be more accurate given that they integrate traits over a larger leaf fraction than 2D estimates, we found that standard 2D anatomical estimations of the relative surface covered by veins over a few leaf cross sections could be accurately used to predict the vein volumetric fraction and, in turn, WUE in conifer leaves (Notes S1; Fig. S4). Stomatal and venation densities covary in angiosperms, directly affecting gas exchange and water use capacities (Carins Murphy *et al.*, 2014). However, conifers do not provide a dense network of veins within the mesophyll to irrigate the photosynthesising cells in water. Consequently, conifers might be constrained to increase the relative volume of veins as a single way to provide more water to the leaf.

Previous work has suggested that narrow, needle-like leaves in conifers, which is a common feature in the Pinaceae (Brodribb &

Feild, 2008; Brodribb *et al.*, 2010), would be a response to alleviate their lack of hydraulic redundancy. With the photosynthetic tissue encircling the single vascular cylinder, the distance from the vein to the epidermis largely sets hydraulic conductance outside the xylem, and mesophyll volume becomes a major limiting factor in cylindrical, narrow leaves. Increasing the radial pathlength for water transport should effectively limit leaf hydraulic conductance, in turn limiting photosynthetic rates (Brodribb *et al.*, 2010). Our data support this hypothesis, with a negative relationship between mesophyll volume and A_{sat} (Fig. S5a). Therefore, within our dataset we found evidence for a significant photosynthetic penalty for increasing leaf width and mesophyll volume in flat and flattened needle leaves (Fig. 3b). With a limited ability to maximise photosynthetic capacity through hydraulic ramification, the cylindrical needle-like leaf may offer opportunities for other structural elements that allow improved hydraulic performance. Accessory transfusion tissue is one of them, where specialised cells connect the veins to the mesophyll tissue, providing more water to the photosynthesising cells and improving hydraulic contact to the epidermis (Brodribb *et al.*, 2007). This might lead to increased photosynthetic rates in needle-like leaves, which presented the most voluminous transfusion tissues (Table S3). Our results support this linkage, with a positive relationship of the combined volumes of transfusion tissue and endoderm with photosynthetic assimilation (Table S5). It has been stated that reaching high photosynthetic rates requires high leaf porosity values, which might increase CO_2 diffusion (Brodribb *et al.*, 2020). Yet, we observed a different trend with a negative relationship between mesophyll porosity and A_{sat} (Table S5). Moreover, A_{sat} was strongly negatively related with V_{mes}/V_{leaf} in our dataset (Fig. S5a). Illumination-induced fluorescence has been shown to be more evenly distributed in needle-like leaves lacking palisade mesophyll layers (Johnson *et al.*, 2005). Therefore, the decrease of A_{sat} in flat leaves with more voluminous mesophylls and often presenting a more differentiated palisade layer might be explained by a limitation of light propagation across the mesophyll. Interestingly, we found conspicuous differences in leaf design between both *Pinus* subgenera and other conifers (Figs 1, 2; Table S4), with narrow needle-leaved *Pinus* possessing less voluminous and porous mesophylls. Such differences in mesophyll construction, which enhance the exchange surface by condensing the mesophyll cells in the more compact mesophyll of needle-like leaves, could explain why A_{sat} is greatest in *Pinus* species.

SA_{mes}/V_{vein} is another feature that has diverged across leaf morphologies and conifer clades (Tables S3, S4). We propose SA_{mes}/V_{vein} as another anatomical trait involved in regulating the control over the loss of water (Fig. 4b). Minimising this ratio would mean that less surface is available for evaporation for a given vein water volume, increasing the time before this capacitor is depleted, and thereby lowering the 'safety margin' between stomatal closure and xylem cavitation (Zwieniecki *et al.*, 2007). Also, in the context of poorly connected hydraulic design, decreasing SA_{mes}/V_{vein} would minimise the apoplastic surface for water to travel from the vein to the epidermis, therefore by proxy decreasing the water path length and increasing connectivity to the epidermis to allow stomata to stay open longer and photosynthesis to continue. In our dataset, decreasing SA_{mes}/V_{vein} was achieved mainly by increasing the relative volume of veins, that is investing more in vascular tissue (Fig. 4). The relative benefit of investing in vein volume to increase the efficiency in water use seems to plateau above *c.* 3% of leaf volume, and most species invest in veins close to that relative volume (Fig. 4a). *Pinus* species, which bear needle-like leaves have, in addition, decreased the relative volume of the mesophyll by decreasing airspace volume (Figs 1, 3a,b, S3a,b) with plicate mesophyll cells (Esau, 1977). Decreasing porosity leads to more cells being in contact with each other, thereby decreasing SA_{mes}, that is the surface of cells exposed to the IAS. Increasing IAS had a positive effect on WUE in six angiosperm species (Mediavilla *et al.*, 2001). Although positive, we could not find a significant relationship between mesophyll porosity and WUE_i in conifer leaves (Table S5). Beyond considering mesophyll features alone, mesophyll volumetrics in interaction with stomatal pore number emerged here as key traits to explain conifer gas exchange and WUE_i (Fig. 5). Using *Arabidopsis* and wheat as model plants, it has been suggested that stomatal differentiation during leaf development might induce mesophyll airspace formation (Lundgren *et al.*, 2019). Our study shows that this coordination between V_{IAS}, along with V_{mes}, and stomatal number have a significant impact on carbon assimilation and gas exchange on conifers (Fig. 5; Table S5), further supporting this crucial linkage. Considered in a wider context, our observations might provide a novel structural basis to explain the lower photosynthetic rates of ferns and gymnosperms compared with angiosperms, as we show that they have greater mesophyll volume per stoma, acting as a bottleneck that limits their evaporative capacities (Fig. S6).

Current increases in temperature and atmospheric CO_2 concentrations might impact the structure and function of conifer forests worldwide, and it has been proposed that improved WUE could alleviate the temperature effect (Brodribb *et al.*, 2020). Previous studies have shown higher WUE_i under increasing CO_2 in conifer species, having stronger WUE_i responses than angiosperms (Dalling *et al.*, 2016; Klein *et al.*, 2016; Adams *et al.*, 2020). Additionally, it has been recently shown that higher plasticity in the vascular tissue of the needles of *Pinus pinaster* enhances their WUE_i (Bert *et al.*, 2021). Using an experimental approach, needles of *Larix kaempferi* growing under higher CO_2 showed increased mesophyll surface area per leaf area, coupled with higher photosynthetic rates (Eguchi *et al.*, 2004). Moreover, it was shown that elevated CO_2 increased mesophyll surface and decreased stomatal density in *Pinus sylvestris* needles (Lin *et al.*, 2001). Therefore, under such elevated CO_2 conditions, we might expect to observe a lower stomata/V_{mes} ratio, which would enhance WUE_i according to our predictions (Fig. 5b). Furthermore, given the recently demonstrated link between enhanced WUE_i and vascular tissue plasticity in conifer needles (Bert *et al.*, 2021), we expect that coordinated changes in vascular and mesophyll tissue volumetrics, along with shifts in stomatal pore number in conifer leaves, may allow conifer species to cope and adapt to the pressure exerted by increasing VPD in many global biomes

(Grossiord *et al.*, 2020) by maintaining similar carbon assimilation levels with lower water consumption.

Acknowledgements

This work was supported by the NSF grants IOS-1626966, IOS-1852976 and IOS-1146746, the Austrian Science Fund (FWF), project M2245, and the Vienna Science and Technology Fund (WWTF), project LS19-013. We thank the Berkeley Arboretum of the University of California Botanical Garden, and the University of Georgia's Thompson Mills Arboretum for providing plant material. The Advanced Light Source is supported by the Director, Office of Science, Office of Basic Energy Science, of the US Department of Energy under contract no. DE-AC02-05CH11231. TNB acknowledges support from the USDA National Institute of Food and Agriculture (Hatch Award 1016439 and Award 2020-67013-30913) and the NSF (IOS-1951244, IOS-1557906).

Author contributions

CB, DMJ, GT-R, ST and TNB designed research; CB, DL, DMJ, GT-R, JME and ST performed measurements and collected data; ST analysed the data and wrote the first draft of the manuscript with major contributions from CB and GT-R. All authors contributed to manuscript revisions.

ORCID

Craig Brodersen https://orcid.org/0000-0002-0924-2570
Thomas N. Buckley https://orcid.org/0000-0001-7610-7136
J. Mason Earles https://orcid.org/0000-0002-8345-9671
Daniel M. Johnson https://orcid.org/0000-0003-1015-9560
David Love https://orcid.org/0000-0002-0582-6990
Guillaume Théroux-Rancourt https://orcid.org/0000-0002-2591-0524
Santiago Trueba https://orcid.org/0000-0001-8218-957X

Data availability

The datasets that support the findings of this study are available as supplementary files.

References

Adams MA, Buckley TN, Turnbull TL. 2020. Diminishing CO_2-driven gains in water-use efficiency of global forests. *Nature Climate Change* **10**: 466–471.

Bert D, Le Provost G, Delzon S, Plomion C, Gion JM. 2021. Higher needle anatomic plasticity is related to better water-use efficiency and higher resistance to embolism in fast-growing *Pinus pinaster* families under water scarcity. *Trees* **35**: 287–306.

Blackmore S, Gibby M, Rae D. 2011. Strengthening the scientific contribution of botanic gardens to the second phase of the Global Strategy for Plant Conservation. *Botanical Journal of the Linnean Society* **166**: 267–281.

Bond WJ. 1989. The tortoise and the hare: ecology of angiosperm dominance and gymnosperm persistence. *Biological Journal of the Linnean Society* **36**: 227–249.

Boyce CK, Brodribb TJ, Feild TS, Zwieniecki MA. 2009. Angiosperm leaf vein evolution was physiologically and environmentally transformative. *Proceedings of the Royal Society B: Biological Sciences* **276**: 1771–1776.

Breshears DD, Carroll CJW, Redmond MD, Wion AP, Allen CD, Cobb NS, Meneses N, Field JP, Wilson LA, Law DJ *et al.* 2018. A dirty dozen ways to die: metrics and modifiers of mortality driven by drought and warming for a tree species. *Frontiers in Forests and Global Change.* doi: 10.3389/ffgc.2018.00004.

Brodribb TJ, Feild TS. 2000. Stem hydraulic supply is linked to leaf photosynthetic capacity: evidence from New Caledonian and Tasmanian rainforests. *Plant, Cell & Environment* **23**: 1381–1388.

Brodribb TJ, Feild TS. 2008. Evolutionary significance of a flat-leaved *Pinus* in Vietnamese rainforest. *New Phytologist* **178**: 201–209.

Brodribb TJ, Feild TS, Jordan GJ. 2007. Leaf maximum photosynthetic rate and venation are linked by hydraulics. *Plant Physiology* **144**: 1890–1898.

Brodribb TJ, Feild TS, Sack L. 2010. Viewing leaf structure and evolution from a hydraulic perspective. *Functional Plant Biology* **37**: 488–498.

Brodribb TJ, McAdam SAM, Jordan GJ, Martins SCV. 2014. Conifer species adapt to low-rainfall climates by following one of two divergent pathways. *Proceedings of the National Academy of Sciences, USA* **111**: 14489–14493.

Brodribb TJ, Pittermann J, Coomes DA. 2012. Elegance versus speed: examining the competition between conifer and angiosperm trees. *International Journal of Plant Sciences* **173**: 673–694.

Brodribb TJ, Powers J, Cochard H, Choat B. 2020. Hanging by a thread? Forests and drought. *Science* **368**: 261.

Carins Murphy MR, Jordan GJ, Brodribb TJ. 2014. Acclimation to humidity modifies the link between leaf size and the density of veins and stomata. *Plant, Cell & Environment* **37**: 124–131.

Carriquí M, Nadal M, Clemente-Moreno MJ, Gago J, Miedes E, Flexas J. 2020. Cell wall composition strongly influences mesophyll conductance in gymnosperms. *The Plant Journal* **103**: 1372–1385.

Choat B, Brodribb TJ, Brodersen CR, Duursma RA, López R, Medlyn BE. 2018. Triggers of tree mortality under drought. *Nature* **558**: 531–539.

Crepet WL, Niklas KJ. 2009. Darwin's second "abominable mystery": why are there so many angiosperm species? *American Journal of Botany* **96**: 366–381.

Dai A. 2011. Drought under global warming: a review. *Wiley Interdisciplinary Reviews: Climate Change* **2**: 45–65.

Dalling JW, Cernusak LA, Winter K, Aranda J, Garcia M, Virgo A, Cheesman AW, Baresch A, Jaramillo C, Turner BL. 2016. Two tropical conifers show strong growth and water-use efficiency responses to altered CO_2 concentration. *Annals of Botany* **118**: 1113–1125.

de Boer HJ, Eppinga MB, Wassen MJ, Dekker SC. 2012. A critical transition in leaf evolution facilitated the Cretaceous angiosperm revolution. *Nature Communications* **3**: 1221.

Earles JM, Buckley TN, Brodersen CR, Busch FA, Cano FJ, Choat B, Evans JR, Farquhar GD, Harwood R, Huynh M *et al.* 2019. Embracing 3D complexity in leaf carbon-water exchange. *Trends in Plant Science* **24**: 15–24.

Earles JM, Théroux-Rancourt G, Roddy AB, Gilbert ME, McElrone AJ, Brodersen C. 2018. Beyond porosity: 3D leaf intercellular airspace traits that impact mesophyll conductance. *Plant Physiology* **178**: 148–162.

Eguchi N, Fukatsu E, Funada R, Tobita H, Kitao M, Maruyama Y, Koike T. 2004. Changes in morphology, anatomy, and photosynthetic capacity of needles of Japanese larch (*Larix kaempferi*) seedlings grown in high CO_2 concentrations. *Photosynthetica* **42**: 173–178.

Esau K. 1977. *Anatomy of seed plants, 2^{nd} edn.* New York, NY, USA: John Wiley & Sons.

Evans JR, Kaldenhoff R, Genty B, Terashima I. 2009. Resistances along the CO_2 diffusion pathway inside leaves. *Journal of Experimental Botany* **60**: 2235–2248.

Felsenstein J. 1985. Phylogenies and the comparative method. *The American Naturalist* **125**: 1–15.

Flexas J, Barbour MM, Brendel O, Cabrera HM, Carriquí M, Díaz-Espejo A, Douthe C, Dreyer E, Ferrio JP, Gago J *et al.* 2012. Mesophyll diffusion conductance to CO_2: an unappreciated central player in photosynthesis. *Plant Science* **193–194**: 70–84.

Freckleton RP, Harvey PH, Pagel M. 2002. Phylogenetic analysis and comparative data: a test and review of evidence. *The American Naturalist* **160**: 712–726.

Gago J, Daloso DM, Carriquí M, Nadal M, Morales M, Araújo WL, Nunes-Nesi A, Flexas J. 2020. Mesophyll conductance: the leaf corridors for photosynthesis. *Biochemical Society Transactions* **48**: 429–439.

Gaylord ML, Kolb TE, Pockman WT, Plaut JA, Yepez EA, Macalady AK, Pangle RE, McDowell NG. 2013. Drought predisposes piñon–juniper woodlands to insect attacks and mortality. *New Phytologist* **198**: 567–578.

Gernandt DS, López GG, García SO, Liston A. 2005. Phylogeny and classification of *Pinus*. *Taxon* **54**: 29–42.

Grossiord C, Buckley TN, Cernusak LA, Novick KA, Poulter B, Siegwolf RTW, Sperry JS, McDowell NG. 2020. Plant responses to rising vapor pressure deficit. *New Phytologist* **226**: 1550–1566.

Guerrieri R, Belmecheri S, Ollinger SV, Asbjornsen H, Jennings K, Xiao J, Stocker BD, Martin M, Hollinger DY, Bracho-Garrillo R *et al.* 2019. Disentangling the role of photosynthesis and stomatal conductance on rising forest water-use efficiency. *Proceedings of the National Academy of Sciences, USA* **116**: 16909.

Gürsoy D, De Carlo F, Xiao X, Jacobsen C. 2014. TomoPy: a framework for the analysis of synchrotron tomographic data. *Journal of Synchrotron Radiation* **21**: 1188–1193.

Hetherington AM, Woodward FI. 2003. The role of stomata in sensing and driving environmental change. *Nature* **424**: 901–908.

Hu Y-S, Yao B-J. 1981. Transfusion tissue in gymnosperm leaves. *Botanical Journal of the Linnean Society* **83**: 263–272.

Johnson DM, Smith WK, Vogelmann TC, Brodersen CR. 2005. Leaf architecture and direction of incident light influence mesophyll fluorescence profiles. *American Journal of Botany* **92**: 1425–1431.

Keenan TF, Hollinger DY, Bohrer G, Dragoni D, Munger JW, Schmid HP, Richardson AD. 2013. Increase in forest water-use efficiency as atmospheric carbon dioxide concentrations rise. *Nature* **499**: 324–327.

Kharuk VI, Im ST, Petrov IA, Dvinskaya ML, Shushpanov AS, Golyukov AS. 2021. Climate-driven conifer mortality in Siberia. *Global Ecology and Biogeography* **30**: 543–556.

Klein T, Bader MKF, Leuzinger S, Mildner M, Schleppi P, Siegwolf RTW, Körner C. 2016. Growth and carbon relations of mature *Picea abies* trees under 5 years of free-air CO_2 enrichment. *Journal of Ecology* **104**: 1720–1733.

Lersten N. 1997. Occurrence of endodermis with a casparian strip in stem and leaf. *The Botanical Review* **63**: 265–272.

Lin J, Jach ME, Ceulemans R. 2001. Stomatal density and needle anatomy of Scots pine (*Pinus sylvestris*) are affected by elevated CO_2. *New Phytologist* **150**: 665–674.

Lundgren MR, Mathers A, Baillie AL, Dunn J, Wilson MJ, Hunt L, Pajor R, Fradera-Soler M, Rolfe S, Osborne CP *et al.* 2019. Mesophyll porosity is modulated by the presence of functional stomata. *Nature Communications* **10**: 2825.

Magallón S, Gómez-Acevedo S, Sánchez-Reyes LL, Hernández-Hernández T. 2015. A metacalibrated time-tree documents the early rise of flowering plant phylogenetic diversity. *New Phytologist* **207**: 437–453.

Martínez-Vilalta J, Sala A, Piñol J. 2004. The hydraulic architecture of Pinaceae – a review. *Plant Ecology* **171**: 3–13.

Mathias JM, Thomas RB. 2021. Global tree intrinsic water use efficiency is enhanced by increased atmospheric CO_2 and modulated by climate and plant functional types. *Proceedings of the National Academy of Sciences, USA* **118**: e2014286118.

McFarlane P, Sands R. 2013. Wood and paper products. In: Sands R, ed. *Forestry in a global context.* Wallingford, UK: CABI Publishing, 77–97.

Mediavilla S, Escudero A, Heilmeier H. 2001. Internal leaf anatomy and photosynthetic resource-use efficiency: interspecific and intraspecific comparisons. *Tree Physiology* **21**: 251–259.

Nobel PS, Zaragoza LJ, Smith WK. 1975. Relation between mesophyll surface area, photosynthetic rate, and illumination level during development for leaves of *Plectranthus parviflorus* Henckel. *Plant Physiology* **55**: 1067.

Orme D, Freckleton R, Thomas G, Petzoldt T, Fritz S, Isaac N. 2018. *CAPER: comparative analyses of phylogenetics and evolution in R.* R package v.1.0.1. [WWW document] URL https://CRAN.R-project.org/package=caper [accessed 25 May 2021].

Paradis E, Schliep K. 2019. APE 5.0: an environment for modern phylogenetics and evolutionary analyses in R. *Bioinformatics* **35**: 526–528.

R Core Team. 2020. *R: a language and environment for statistical computing.* Vienna, Austria: R Foundation for Statistical Computing.

Schmiege SC, Buckley BM, Stevenson D, Cuong TQ, Nam LC, Griffin KL. 2020. Contrasting physiological traits of shade tolerance in *Pinus* and Podocarpaceae native to a tropical Vietnamese forest: insight from an aberrant flat-leaved pine. *Tree Physiology* **41**: 223–239.

Schmiege SC, Buckley BM, Stevenson DW, Heskel MA, Cuong TQ, Nam LC, Griffin KL. 2021. Respiratory temperature responses of tropical conifers differ with leaf morphology. *Functional Ecology* **35**: 1408–1423.

Schneider CA, Rasband WS, Eliceiri KW. 2012. NIH Image to IMAGEJ: 25 years of image analysis. *Nature Methods* **9**: 671–675.

Smith SA, Brown JW. 2018. Constructing a broadly inclusive seed plant phylogeny. *American Journal of Botany* **105**: 302–314.

Smith WK, Nobel PS. 1977. Influences of seasonal changes in leaf morphology on water-use efficiency for three desert broadleaf shrubs. *Ecology* **58**: 1033–1043.

Théroux-Rancourt G, Earles JM, Gilbert ME, Zwieniecki MA, Boyce CK, McElrone AJ, Brodersen CR. 2017. The bias of a two-dimensional view: comparing two-dimensional and three-dimensional mesophyll surface area estimates using noninvasive imaging. *New Phytologist* **215**: 1609–1622.

Théroux-Rancourt G, Jenkins MR, Brodersen CR, McElrone A, Forrestel EJ, Earles JM. 2020. Digitally deconstructing leaves in 3D using X-ray microcomputed tomography and machine learning. *Applications in Plant Sciences* **8**: e11380.

Théroux-Rancourt G, Roddy AB, Earles JM, Gilbert ME, Zwieniecki MA, Boyce CK, Tholen D, McElrone AJ, Simonin KA, Brodersen CR. 2021. Maximum CO_2 diffusion inside leaves is limited by the scaling of cell size and genome size. *Proceedings of the Royal Society B: Biological Sciences* **288**: 20203145.

Warton DI, Duursma RA, Falster DS, Taskinen S. 2012. SMATR 3 – an R package for estimation and inference about allometric lines. *Methods in Ecology and Evolution* **3**: 257–259.

Zwieniecki MA, Boyce CK, Holbrook NM. 2004. Functional design space of single-veined leaves: role of tissue hydraulic properties in constraining leaf size and shape. *Annals of Botany* **94**: 507–513.

Zwieniecki MA, Brodribb TJ, Holbrook NM. 2007. Hydraulic design of leaves: insights from rehydration kinetics. *Plant, Cell & Environment* **30**: 910–921.

Supporting Information

Additional Supporting Information may be found online in the Supporting Information section at the end of the article.

Dataset S1 Species averaged values of volumetric anatomy and stomatal traits of conifer leaves.

Dataset S2 Phylogeny of 34 studied conifer species.

Dataset S3 Metadata of volume-based stomatal density.

Fig. S1 Phylogenetic relationships across the 34 studied species.

Fig. S2 Proportion of tissue relative volumes inside the 3D leaf space for the 34 conifer species studied.

Fig. S3 Comparison of leaf 3D structure across conifer groups.

Fig. S4 Comparison between 2D area fractions and 3D volumetric fractions in conifer leaf veins.

Fig. S5 Light-saturated photosynthetic assimilation (A_{sat}) as a function of volumetric anatomy and stomatal traits in conifers.

Fig. S6 Stomatal number per mesophyll volume across vascular plant groups.

Notes S1 Comparing 2D area fractions to 3D volumetric fractions.

Table S1 Abbreviations and definitions of anatomical and gas exchange variables measured, with reference to their units.

Table S2 Structural coordination within the volumetric space of the conifer leaf.

Table S3 Comparisons of volumetric anatomy and stomatal traits across different leaf morphologies in conifers.

Table S4 Comparisons of volumetric anatomy and physiological features between *Pinus* subgenera *Pinus* and *Strobus*, and other conifer species.

Table S5 Variation in gas exchange, photosynthesis and water use efficiency as explained by leaf volumetric anatomy and stomatal traits.

Please note: Wiley Blackwell are not responsible for the content or functionality of any Supporting Information supplied by the authors. Any queries (other than missing material) should be directed to the *New Phytologist* Central Office.

About *New Phytologist*

- *New Phytologist* is an electronic (online-only) journal owned by the New Phytologist Foundation, a **not-for-profit organization** dedicated to the promotion of plant science, facilitating projects from symposia to free access for our Tansley reviews and Tansley insights.
- Regular papers, Letters, Viewpoints, Research reviews, Rapid reports and both Modelling/Theory and Methods papers are encouraged. We are committed to rapid processing, from online submission through to publication 'as ready' via *Early View* – our average time to decision is <26 days. There are **no page or colour charges** and a PDF version will be provided for each article.
- The journal is available online at Wiley Online Library. Visit **www.newphytologist.com** to search the articles and register for table of contents email alerts.
- If you have any questions, do get in touch with Central Office (np-centraloffice@lancaster.ac.uk) or, if it is more convenient, our USA Office (np-usaoffice@lancaster.ac.uk)
- For submission instructions, subscription and all the latest information visit **www.newphytologist.com**

© 2021 The Authors
New Phytologist © 2021 New Phytologist Foundation